A microfabricated array of clamps for immobilizing and imaging *C. elegans*

S. Elizabeth Hulme,[a] Sergey S. Shevkoplyas,[a] Javier Apfeld,[b] Walter Fontana*[b] and George M. Whitesides*[a]

Received 25th May 2007, Accepted 24th July 2007
First published as an Advance Article on the web 16th August 2007
DOI: 10.1039/b707861g

This paper describes the fabrication of a microfluidic device for rapid immobilization of large numbers of live *C. elegans* for performing morphological analysis, microsurgery, and fluorescence imaging in a high-throughput manner. The device consists of two principal elements: (i) an array of 128 wedge-shaped microchannels, or clamps, which physically immobilize worms, and (ii) a branching network of distribution channels, which deliver worms to the array. The flow of liquid through the device (driven by a constant pressure difference between the inlet and the outlet) automatically distributes individual worms into each clamp. It was possible to immobilize more than 100 worms in less than 15 min. The immobilization process was not damaging to the worms: following removal from the array of clamps, worms lived typical lifespans and reproduced normally. The ability to monitor large numbers of immobilized worms easily and in parallel will enable researchers to investigate physiology and behavior in large populations of *C. elegans*.

Introduction

This paper describes the fabrication of a microfluidic device for rapid immobilization of large numbers (>100, with the potential to expand to larger numbers) of live *C. elegans*. The procedure requires less than 15 min, and distributes the worms into an array of individual wedge-shaped channels, which we call clamps. These clamps restrain the worms for high-resolution optical imaging. When compared to existing methods for immobilization, the microfluidic worm clamp reduces the chemical and mechanical stress that immobilization places on a worm. In addition, because our device immobilizes multiple worms at once, it should decrease the amount of time needed to collect data on large numbers of worms.

Studies of *C. elegans* often require that worms remain immobile during observation. Experiments such as (i) detailed structural analysis of anatomical features of the worm (for example, the shape of the pharynx[1] or the structure of the muscles of the body[2]), (ii) microsurgical ablation of tissues using nano- or femtosecond laser pulses,[3–5] and (iii) acquisition of high-resolution time-series with fluorescent probes (for example, for indirectly monitoring neuronal responses to stimuli)[6–8] all require that worms remain still (or at least within the field of view of a microscope) for the duration of the procedure.

There are currently two commonly-used methods for immobilizing *C. elegans*: (i) gluing the worm to an agarose pad using a cyanoacrylate glue,[7,9,10] or (ii) treating the organism with drugs, such as sodium azide (a metabolic inhibitor)[11] or levamisole (a cholinergic agonist).[12] The first method—gluing the worm—takes approximately two minutes per worm (in our experience); in order to examine a large number of worms, researchers must devote substantial time during an experiment to immobilizing the animals. In addition, the adhesion of the glue to the worm is not reversible: once a worm has been glued, it is not possible to release it, and the monomers in the glue are likely to have some toxicity. The second method—treatment with paralytic drugs—is useful for paralyzing (and, in this sense, immobilizing) very large numbers of worms at once, but has the disadvantage that it unavoidably changes the internal biochemical state of the worm during the procedure. Less commonly, researchers have used micropipettes to immobilize individual animals by holding either the head or the tail of a worm in place inside the micropipette using suction.[13,14] A major limitation of this procedure is that (as with the gluing method) it is only possible to immobilize and examine one worm at a time.

Several groups have recently proposed microfluidic systems for observing *C. elegans*;[15–17] however, these systems have been designed either for imaging worms that are not immobilized at low-resolution,[15,16] or for imaging worms that have been paralyzed, or even euthanized, at high-resolution.[17] To improve upon existing methods for immobilizing worms, we have developed a microfluidic device that is capable of immobilizing over 100 worms at once. The device consists of a network of distribution channels, which deliver worms to an array of wedge-shaped microfluidic channels, or clamps. The geometry of the clamps is such that the worms fit snugly inside the wedge-shaped channels; the clamps physically prevent the worms from moving.

A major advantage of this new tool is that one can immobilize over 100 worms in less than 15 min. This procedure reduces the amount of time that would otherwise be needed to immobilize the same number of worms using the gluing method by more than an order of magnitude. Because the immobilization of worms within microfluidic clamps does not involve treatment with drugs, or any other invasive measures, it avoids disruption of the natural biochemical state of the worm. By reversing the direction of flow in the device, one may

[a]*Department of Chemistry and Chemical Biology, Harvard University, 12 Oxford St., Cambridge, MA, 02141, USA. E-mail: gwhitesides@gmwgroup.harvard.edu*
[b]*Department of Systems Biology, Harvard Medical School, 200 Longwood Ave., Boston, MA, 02115, USA. E-mail: walter@hms.harvard.edu*

release the worms from the clamps; repeated sampling of the same population of worms at different times is therefore possible. The ability to immobilize many worms in a single device should enable researchers to perform highly parallel experiments on large populations of worms. In principle, this method could be extended to immobilize much larger numbers of worms.

Experimental design

Design of the worm clamp

The body of *C. elegans* has the shape of an elongated cylinder that tapers at both the head and tail ends. As Fig. 1a shows, an adult worm is approximately 1.2 mm long and 50–60 μm wide.[18] In order to crawl forward on a surface or to swim in a liquid environment, *C. elegans* contracts and relaxes a set of dorsal-ventral muscles to produce a coordinated sinusoidal motion along its body[19] (the worm shown in Fig. 1a is crawling towards the upper right-hand corner of the image). On an agar surface, an adult worm crawls at a rate of approximately 200 μm—roughly 20% of the length of its body—per second.[20] This velocity makes it technically difficult (though not impossible[21,22]) to track the movement of a worm at high magnification. (Detailed observation of *C. elegans* often requires a magnification of 50× or more.[3,4,6,21,22])

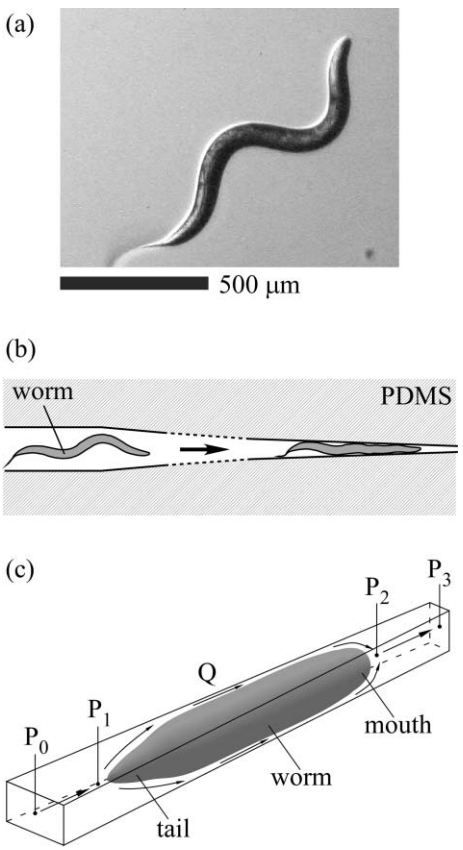

Fig. 1 Design of the worm clamp. (a) *C. elegans* crawling freely (towards the upper right-hand corner of the image). The worm in this image is approximately 1.2 mm long and 50–60 μm wide. (b) Schematic illustration of the microfluidic worm clamp. The worm clamp consists of a tapered microfluidic channel—constructed in PDMS—that is designed to restrain the motion of a worm. A pressure difference applied across the inlet and outlet drives the flow of liquid through the device. The resulting pressure-driven flow carries the worm into the wedge-shaped microchannel (the clamp) until the worm fits snugly within the channel. (c) Schematic illustration of a worm immobilized within a single worm clamp. The pressure along the clamp decreases from P_0 at the inlet, to P_1 at the tail of the worm, to P_2 at the head of the worm, and finally, to P_3 at the outlet of the clamp. A constant pressure difference across the inlet and the outlet of the device ($\Delta P \equiv P_0 - P_3$ = const) is used to drive the flow of liquid through the device. The volumetric rate of flow through the device is represented by Q.

Our approach for immobilizing *C. elegans* was to capture individual worms inside of wedge-shaped microchannels with cross-sectional dimensions similar in size to the cross-sectional diameter of a worm. Each worm is held in place by the geometry of the clamp: the walls of the channel prevent any sinusoidal motion along the body of the worm and thus prevent the worm from crawling or swimming in the microchannel. Fig. 1b illustrates this approach. A similar method has previously been used to trap human erythrocytes.[23,24]

Constant pressure *versus* constant flow

We used a constant pressure difference between the inlet and the outlet of the device to drive the flow of liquid (and along with the flow, worms) from the inlet into the device, and to hold the worms in place in the clamps. Fig. 1c shows a schematic diagram of the distribution of pressure along a wedge-shaped microchannel containing a worm. (We have analyzed a related problem—the pressure drop along rectangular microchannels containing bubbles—previously in detail.[25])

The distribution of pressure along a single worm clamp (Fig. 1c) is governed by a system of equations (eqn (1)), where P_0 is the pressure at the inlet, P_1 is the pressure at the tail of the worm, P_2 is the pressure at the mouth of the worm, P_3 is the pressure at the outlet, R_{01} is the resistance of the inlet part of the channel, R_{12} is the resistance of the part of the channel containing the immobilized worm, R_{23} is the resistance of the outlet part of the channel, and Q is the volumetric flow rate of liquid through the clamp.

$$\begin{cases} P_0 - P_1 = R_{01}Q \\ P_1 - P_2 = R_{12}Q \\ P_2 - P_3 = R_{23}Q \end{cases} \quad (1)$$

If the pressure difference driving the flow of liquid through the system is kept constant ($\Delta P \equiv P_0 - P_3$ = const), the pressure drop across the worm is given by eqn (2).

$$P_1 - P_2 = \frac{R_{12}}{R_{01} + R_{12} + R_{23}}(P_0 - P_3) \quad (2)$$

The presence of the worm in the wedge-shaped channel increases the resistance of the channel (the worm plugs the channel)—the better the worm conforms to the shape of the clamp, the higher the resistance of the part of the channel containing the worm (that is, ultimately, $R_{12} \to \infty$). In this case, the pressure difference to which the worm is subjected can never exceed the driving pressure ($\Delta P \equiv P_0 - P_3$) applied

to the whole system (eqn (3)).

$$\lim_{R_{12}\to\infty}(P_1-P_2)=\lim_{R_{12}\to\infty}\left(\frac{1}{1+\dfrac{R_{01}+R_{23}}{R_{12}}}(P_0-P_3)\right)=(P_0-P_3) \quad (3)$$

If, alternatively, the volumetric flow rate of the liquid through the system is kept constant (Q = const), then the pressure gradient across the worm is given by eqn (4).

$$P_1 - P_2 = R_{12}Q \quad (4)$$

As the resistance of the channel increases ($R_{12} \to \infty$), due to the presence of the worm, the pressure gradient across the worm rises without bound (eqn (5)). The unbounded increase in pressure that would result from the operation of the device in the regime of constant flow could cause significant mechanical damage to the immobilized worm: a large pressure gradient across the worm could potentially rupture its cuticle. By choosing to operate the device in the regime of constant pressure, we place an upper limit on the pressure gradient across the worm immobilized within the clamp.

$$\lim_{R_{12}\to\infty}(P_1 - P_2) = \lim_{R_{12}\to\infty}(R_{12}Q) = \infty \quad (5)$$

Design of an array of multiple worm clamps

Fig. 2a shows the actual design of a single worm clamp. The width of the microchannel narrows gradually—from 100 μm to 10 μm—over a length of 5 mm. We designed the channels to taper gradually to accommodate worms of varying sizes; natural variation in diameter and length exist even within isogenic populations of worms.

In order to immobilize many worms in a single device, we created a microfluidic array of the individual worm clamps. Fig. 2b shows the design of an array of four clamps, with a network of distribution channels leading to, and from, the clamps.

The network of channels that deliver the worms from the inlet to the clamps contains only bifurcated branching points. It is straightforward to increase the number of clamps (2^N) in the array by increasing the number of bifurcation points (N). We chose bifurcations (as opposed to trifurcations, or even higher order branching topologies) because it is straightforward to design downstream branches of identical fluidic resistance for each of the branching points in the network. This design prevents any bias in the distribution of worms due to geometry, and also ensures that if the total driving pressure across the device is constant, the pressure drop across each worm immobilized within the clamps should be approximately the same.

Distribution of the worms in an array of four clamps

At each bifurcation, or decision point, in the network of inlet channels, the path of the worm is determined by the ratio of the flow rates into the two downstream branches. In order to analyze the distribution of flow through the array of four clamps, it is useful to represent the array (with the accompanying distribution channels from the inlet and to the outlet) as a branched network of fluidic resistors (Fig. 2c). The distribution of pressure throughout the array shown in

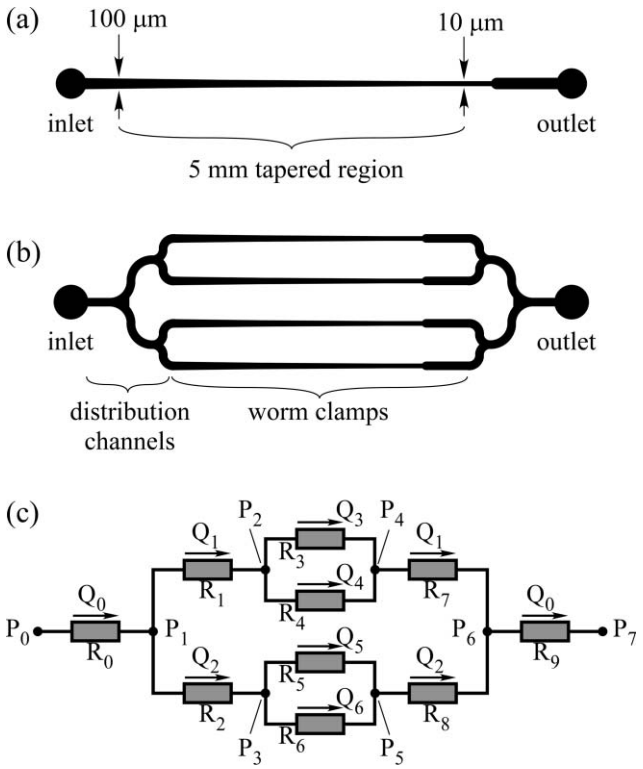

Fig. 2 Design of an array of worm clamps. (a) Design of a single worm clamp. (b) Design of an array of four worm clamps. The array is designed such that, on average, one worm is sorted into each clamp. The diagrams in (a) and (b) are not drawn to scale in the vertical direction. (c) Analysis of the distribution of flow through an array of four worm clamps. The four clamps (with the accompanying distribution channels from the inlet and the outlet) are represented as a branched network of fluidic resistors (R_0 through R_9). Each resistive segment of the network has a corresponding volumetric rate of flow (Q_0 through Q_9), and each branching point has an associated pressure (P_0 through P_7).

Fig. 2c is given by a system of algebraic equations (eqn (6)).

$$\begin{cases} P_0-P_1=Q_0R_0 \\ P_1-P_2=Q_1R_1 \\ P_1-P_3=Q_2R_2 \\ P_2-P_4=Q_3R_3=Q_4R_4 \end{cases} \quad \begin{cases} P_3-P_5=Q_5R_5=Q_6R_6 \\ P_4-P_6=Q_1R_7 \\ P_5-P_6=Q_2R_8 \\ P_6-P_7=Q_0R_9 \end{cases} \quad (6)$$

$$\begin{cases} Q_0=Q_1+Q_2 \\ Q_1=Q_3+Q_4 \\ Q_2=Q_5+Q_6 \end{cases}$$

We solve this system (eqn (6)) to find the flow rates throughout the device (eqn (7), (8) and (9)). These relationships help us to explain the dynamics of the distribution of worms throughout the device as it is being filled with worms.

Eqn (7) show the ratios of the flow rates at the decision points corresponding to P_2 and P_3.

$$\begin{cases} \dfrac{Q_3}{Q_4}=\dfrac{R_4}{R_3} \\ \dfrac{Q_5}{Q_6}=\dfrac{R_6}{R_5} \end{cases} \quad (7)$$

In an empty device, the flow rates through the clamp corresponding to R_3 and the clamp corresponding to R_4 are equal, because the fluidic resistances of the clamps are equal. Under these conditions, a worm at the decision point P_2 has an equal chance of taking the path to clamp R_3 or to clamp R_4. Once a worm occupies, for instance, clamp R_3, the balance of the flow rates changes—the flow through clamp R_3 diminishes and the flow through clamp R_4 increases (eqn (7)). The next worm to arrive at the decision point P_2 will, therefore, likely take the path to clamp R_4. (While the ratio of the flow rates dominates this decision, other factors—such as the voluntary swimming motion of the body of the worm, the inertia of the worm, the geometry of the decision point, and defects in the fabrication of the device—may affect the actual outcome.) The distribution process at P_3 is identical to the process at point P_2.

Eqn (8) shows the ratio of flow rates into the downstream branches at decision point P_1.

$$\frac{Q_1}{Q_2} = \frac{R_2 + R_8 + \dfrac{R_5 R_6}{R_5 + R_6}}{R_1 + R_7 + \dfrac{R_3 R_4}{R_3 + R_4}} \tag{8}$$

The dynamics of the distribution of worms at the decision point P_1 are slightly more complicated than at point P_2, because the ratio of the flow rates depends not only on the occupancy of the clamps, but also on the presence of the worms in the distribution channels leading up to the clamps (eqn (8), Fig. 2c). (The clamps prevent worms from ever reaching the channels leading from the clamps to the outlet.) The presence of worms in the distribution channels downstream of decision point P_1 increases the resistance of these channels and the branches that these channels comprise, and causes the next worm that reaches the decision point to select the other branch.

The total flow through the four-clamp device (Fig. 2c) is given by eqn (9).

$$Q_0 = \frac{(P_0 - P_7)}{R_0 + R_9 + \dfrac{\left(R_1 + R_7 + \dfrac{R_3 R_4}{R_3 + R_4}\right)\left(R_2 + R_8 + \dfrac{R_5 R_6}{R_5 + R_6}\right)}{\left(R_1 + R_2 + R_7 + R_8 + \dfrac{R_3 R_4}{R_3 + R_4} + \dfrac{R_5 R_6}{R_5 + R_6}\right)}} \tag{9}$$

If the driving pressure ($\Delta P \equiv P_0 - P_7$) remains fixed, it follows from eqn (9) that as the clamps become filled with worms (R_3, R_4, R_5, and R_6 increase), the total flow through the system decreases (eqn (9)).

The presence of a worm within a clamp significantly reduces (or even completely obstructs) the flow of liquid through that clamp. This reduction in flow diverts subsequent worms at the upstream branching points into the other clamps. Thus by design, the device loads a given clamp with only one worm. As more clamps become occupied by worms, the total flow of liquid through the device decreases, and the clamps fill with worms progressively slower.

Using soft lithography to fabricate the array of worm clamps

We fabricated the microfluidic array of worm clamps out of poly(dimethyl siloxane) (PDMS) using soft lithography.[26–28] Because PDMS is optically transparent at wavelengths above 230 nm,[28] it is compatible with the majority of imaging applications. PDMS is relatively mechanically compliant, permeable to oxygen and carbon dioxide, and non-toxic;[29,30] these properties make it an especially useful material for constructing devices that are compatible with living organisms.[26,31,32] Soft lithography has the additional advantage that a large number of microfluidic components and analytical tools—such as microelectrodes,[33] valves,[34,35] and lasers[36]—have previously been developed for use with PDMS devices. It would be possible to incorporate these components into future versions of the device.

Results and discussion

The immobilization device: an array of 128 worm clamps

By increasing the number of bifurcations from two to seven, we were able to design an array of 128 worm clamps. Fig. 3a shows the design for this 128-clamp device.

We fabricated the devices using soft lithography.[28] The height of all of the channels in the device was 55 μm. The inlet and outlet ports were constructed by punching 1.5 mm holes through the PDMS devices using biopsy punches. Devices were exposed to an oxidizing air plasma and sealed, either to a plasma-oxidized glass slide (50 × 75 mm, 1.2 mm thick), or to a plasma-oxidized glass coverslip (48 × 65 mm, No. 1 thickness) to enable imaging using objectives with short working distances (objectives with high magnifying power). Devices were filled with M9 buffer[37] and placed under vacuum (−95 kPa, or −0.94 atm, relative to the atmosphere) in a vacuum desiccator for 10 min to remove any bubbles present in the microfluidic channels.

Fig. 3b shows an illustration of the experimental set-up. Flow through the device was driven by vacuum suction: a pressure difference across the device was created by attaching the outlet of the device to a source of vacuum (−95 kPa, or −0.94 atm, relative to the atmosphere) *via* polyethylene tubing (PE-205). An inlet reservoir, consisting of a glass Pasteur pipette connected to the inlet of the device *via* polyethylene tubing (PE-205), served as the loading port for the M9 buffer and the suspension of worms.

Preparation of synchronous worms

We obtained a synchronous population of young adult worms using an established method.[37] Briefly, we transferred approximately 25 gravid (egg-containing) adult worms from a bacterial lawn into a small volume (0.5 mL) of a 1 : 1 mixture of 1 M sodium hydroxide and sodium hypochlorite. Within 10 min, the alkaline hypochlorite solution had dissolved the bodies of the adult worms; the developing embryos within the adult worms, however, were protected from damage by their chitinous shells.[38]

On average, each adult worm released 5–10 embryos. The embryos were washed into M9 buffer and incubated, without food, overnight at 20 °C. In the absence of food, embryos of *C. elegans* will hatch and then arrest growth early in the first larval stage (L1);[39] in this way, we created a synchronous population of starved L1 animals. We transferred the synchronized L1 worms onto nematode growth

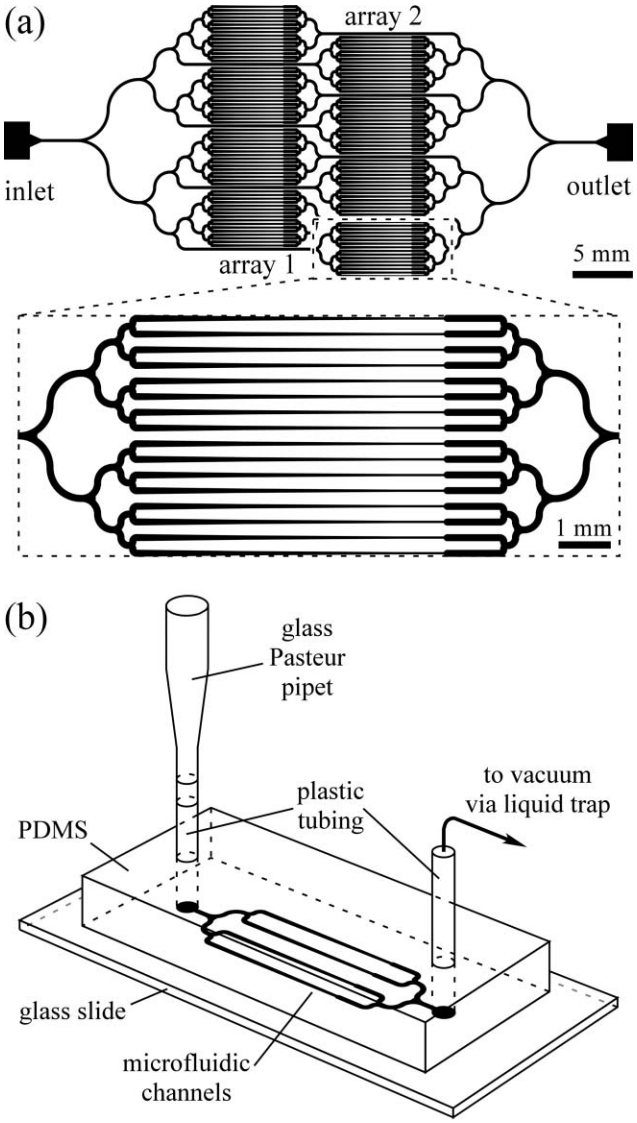

Fig. 3 The worm clamp device. (a) Design of an array of 128 worm clamps; the inset is a magnified view of the array, showing 16 of the 128 clamps. The diagrams are not to scale in the vertical direction. (b) Experimental set-up for the worm clamp device. Devices were made of PDMS using soft lithography. An inlet reservoir was constructed by connecting a glass Pasteur pipette to the inlet of the device using a 2 cm long piece of polyethylene tubing. The inlet reservoir provided a loading point for introducing a suspension of worms into the device. Connection of polyethylene tubing at the outlet of the device to a source of vacuum (−95 kPa, or −0.94 atm, relative to the atmosphere) through a liquid trap (not shown) created a pressure difference across the device, and produced the flow of liquid through the device.

media (NGM) agar plates that had been seeded with *E. coli*. After 45 h at 20 °C, the synchronized worms had grown into young adult animals.

Loading worms into the 128-clamp device

To prepare the worms for loading into the device, we washed them from the NGM plates using 2 mL of M9 buffer, and transferred the suspension to a conical centrifuge tube. To remove bacteria from this suspension, we allowed the adult worms to settle to the bottom of the tube, aspirated the supernatant liquid, and resuspended the worms in fresh M9 buffer. The concentration of worms in the suspension was approximately 100 worms mL^{-1}.

To initiate loading, 0.5 mL of the suspension of worms was added to the reservoir at the inlet of the device, and the vacuum at the outlet was turned on. Immediately, the flow of liquid carried worms into the device. Additional worms were added to the reservoir at the inlet as needed. Within 15 min, nearly every clamp in the device contained a worm.

Fig. 4 shows the result of a typical experiment following the addition of worms to the 128-clamp device. In total, 116 worms were successfully immobilized within the array of clamps; that is, over 90% of the clamps contained a single, immobilized worm. Occasionally, two or more worms entered a single clamp; the incidence of these 'doubles,' however, was low enough that it did not significantly detract from the success rate of the device. For the experiment shown in Fig. 4, there was only one clamp that contained two worms.

Some of the clamps did not contain any worms (11 of the clamps shown in Fig. 4 are empty). As described by eqn (9) in the Experimental design section, the cause of these empty clamps was a decrease in the overall rate of flow at the inlet of the device as the clamps became populated with worms, due to the increase of the total fluidic resistance of the device. Despite the fact that some of the clamps remained empty, the success rate of the device was sufficiently high to immobilize over 100 worms in less than 15 min.

From the images in Fig. 4, it is apparent that the worms do not all reach the same position along the clamps; instead, there is a distribution of positions. This distribution is due to the natural variation in size of the individual worms in a synchronous population of worms. We quantified this distribution by measuring the length of each worm within the immobilization device. The mean length of the worms shown in Fig. 4 is (1.2 ± 0.1) mm.

We found that the worms immobilized in the 128-clamp device were not all oriented in the same direction. We observed a weak bias towards the head-first orientation (63 out of 116 worms) over the tail-first orientation (53 out of 116 worms). We did not observe any correlation between the orientation of a worm and the position of that worm in the clamp. Fig. 5 shows a series of increasingly magnified views of worms within the 128-clamp array. Anatomical features of *C. elegans*—such as the mouth, pharynx, developing embryos, unfertilized oocytes, and the tail—are observable at high magnification.

Releasing the worms from the 128-clamp device

In order to remove the worms from the clamps, we manually applied pressure to a buffer-filled syringe connected to the outlet of the device to reverse the direction of flow through the device, and collected the worms from the inlet in a suspension of M9 buffer. During the removal process, one worm remained trapped inside the device; however, we were able to extract all of the other worms from the device successfully.

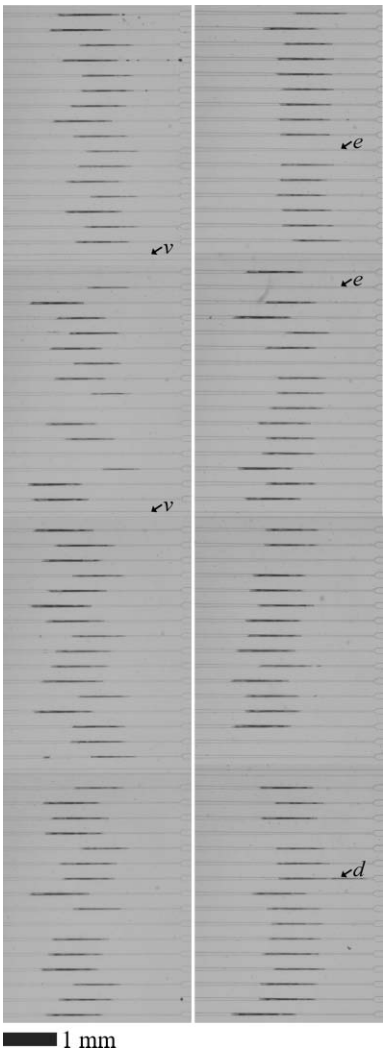

Fig. 4 Composite image of worms immobilized within the 128-clamp device. Pressure-driven flow was used to introduce a synchronous population of worms into the device. The left panel corresponds to array 1 in Fig. 3a; the right panel corresponds to array 2 in Fig. 3a. Out of 128 clamps, 116 of the clamps contained a single, immobilized worm, 1 of the clamps contained more than one worm (a 'double'), and 11 of the clamps were empty. The symbols *v*, *e*, and *d* indicate vias (distribution channels), empty clamps, and doubles (clamps with two worms), respectively. The orientation of the worms appears to be weakly biased towards the head-first orientation: of the 116 immobilized worms, 63 are oriented head-first, and 53 are oriented tail-first. The average length of the immobilized worms is (1.2 $\pm$ 0.1) mm.

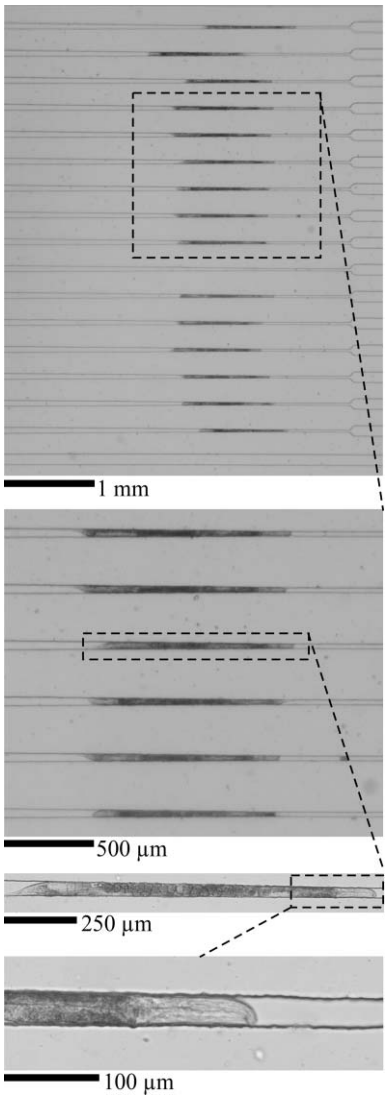

Fig. 5 A series of magnified views of worms immobilized in the 128-clamp device.

Monitoring the survival of worms following release from the device

We had anticipated that any damage sustained by the worms during the immobilization process would be mechanical damage to either the outer cuticle or to the internal anatomical structures of the worm. In *C. elegans*, damage to the cuticle is readily observable as a loss of pressure in the body of the worm. The turgid shape of the body of *C. elegans* is maintained by high osmotic pressure within the cuticle of the worm.[40] If the cuticle surrounding the outside of the worm becomes damaged, the internal turgor pressure will decrease, thus diminishing the ability of the worm to move. Significant damage to the cuticle will cause a total loss of turgor pressure, and will result in the death of the animal.[40,41]

Additionally, damage to certain internal anatomical structures of the worm would likely be apparent after releasing the worms from the immobilization device. For example, damage to the reproductive system, the somatic muscles, or the gut (the pharynx and intestine) would be observable in the worm as a reduced ability to produce progeny, to crawl, or to eat, respectively.

In order to demonstrate that the immobilization process did not noticeably damage the worms, we monitored the behavior, survival, and progeny-production of a subset of worms following their removal from the clamps. We randomly selected 21 worms from the more than 100 worms that had been released from the device. We placed the worms on an NGM plate that had been seeded with *E. coli*, and incubated the worms at 20 °C. Upon visual inspection, the bodies of the worms did not appear to be diminished in turgor pressure, and they were crawling and feeding normally (Fig. 6b).

During the first week of observation, we transferred the worms to fresh plates each day in order to separate the worms from their progeny. We monitored survival each day by prodding each worm with a platinum wire and observing whether or not the worm moved in response to the prod. Worms that did not move were scored as dead.[41] Fig. 6c contrasts a live worm (Fig. 6c,i) with a dead worm (Fig. 6c,ii) at day 16 of the lifespan study. The mean lifespan of the worms was (15 ± 5) days, which was in agreement with the literature[42] value for the mean lifespan of a population of healthy worms at 20 °C. Fig. 6a shows the survival curve for the population.

We also monitored the production of progeny in a separate group of 4 worms that had been randomly selected after being removed from the device. In agreement with observations in the literature,[42] each worm produced hundreds of progeny over a 6 day period.

Based on these data, we concluded that the process of introducing the worms into the clamps, immobilizing them, and releasing them from the device does not cause significant damage to the worms.

Conclusions

The array of worm clamps described here rapidly immobilizes over 100 worms at once. This device should allow researchers of *C. elegans* to perform morphological analysis, microsurgery, and fluorescence imaging in high-throughput experiments. The ability to monitor large numbers of immobilized worms rapidly and in parallel will enable researchers to investigate natural variations in the physiology and behavior of large populations of *C. elegans*. In principle, the immobilization device could also be useful for the identification of certain types of mutant phenotypes in forward genetic screens;[43] in particular, the device should be useful for identifying mutations affecting anatomical structure or body size.

With the current design, the clamps themselves can be used as analytical devices to measure the size distribution of a population of worms. The ability to measure size easily is potentially useful for monitoring the effects of genetic perturbations and/or environmental conditions on body size.

Modifications to the current design could introduce new capabilities. Because this approach for immobilizing worms uses microchannels, it should be possible to introduce additional microfluidic components that would enable the delivery of solutions of chemicals to the worms during immobilization. It should also be possible to subject immobilized worms to other forms of external stimuli, such as light, mechanical stress, or electrical stimulation. In addition, because the immobilization device creates an ordered array of immobilized worms, it should be possible to automate the acquisition of data using a motorized microscope stage.

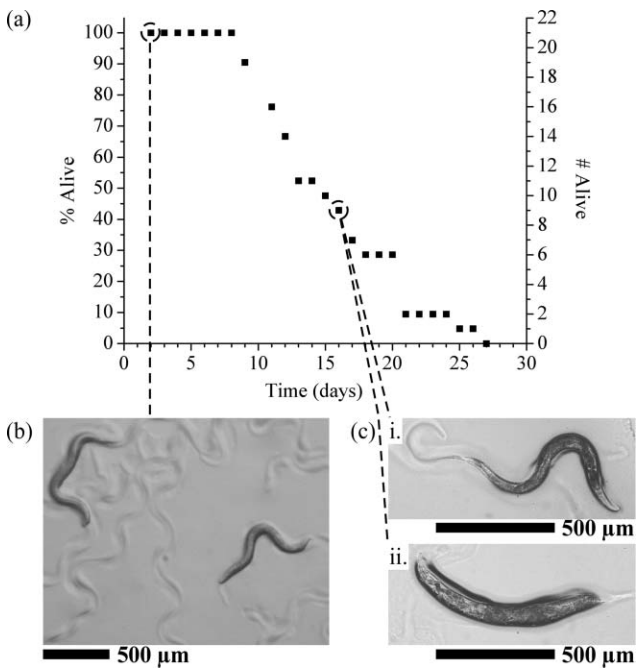

Fig. 6 Survival of worms following immobilization within the array of 128 clamps. (a) Lifespan curve for a sample of 21 worms following removal from the 128-clamp device. Worms were monitored each day and scored as alive or dead. Each point in the lifespan curve represents the percentage of the initial population of 21 worms that are still alive on that day. Worms were hatched from eggs on day 0, and were immobilized within the 128-clamp device on day 2. The average lifespan of the worms was (15 ± 5) days. (b) Freely crawling worms on day 2, following removal from the 128-clamp device. Worms were crawling and feeding normally. (c) Worms on day 16. Some worms appeared healthy (i), while others appeared bloated and lacked motility (ii).

Experimental

Materials

All reagents were purchased from Sigma or VWR unless otherwise stated. NGM was prepared by mixing 3 g NaCl, 17 g Bacto™ agar, and 2.5 g Bacto™ peptone into 975 mL of water. The mixture was autoclaved for 1 h and cooled to 55 °C. Following the autoclaving step, 1 mL 1 M $CaCl_2$, 1 mL of a solution of cholesterol (5 mg mL^{-1} in ethanol), 1 mL 1 M $MgSO_4$ and 25 mL 1 M KPO_4 buffer (0.8 M KH_2PO_4, 0.2 M K_2HPO_4, adjusted to pH 6.0) were added to the solution. Aliquots (11 mL) of the NGM solution were dispensed into 60 mm petri dishes and stored at 4 °C. M9 buffer was prepared by combining 3 g KH_2PO_4, 6 g Na_2HPO_4, 5 g NaCl and 1 mL 1 M $MgSO_4$, and adding H_2O to 1 L. The buffer was sterilized by autoclaving. All experiments were performed in compliance with the guidelines set forth by Harvard University's Institutional Animal Care and Use Committee (IACUC).

Fabrication of PDMS devices

The design of the 128-clamp device, shown in Fig. 3, contained 128 clamps, organized into 8 groups of 16 clamps. Within each group, the clamps were arrayed at a spacing of 300 μm. Each clamp consisted of a 5 mm long tapered segment, which tapered from 100 μm to 10 μm in width, followed by a 1 mm long segment that was 10 μm in width, and subsequently followed by a 1 mm long segment that was 100 μm in width. In the design of the branching inlet and outlet channels, each curved segment was made up of two, equally sized, quarter-circles, with a thickness of 100 μm. The radii of curvature of the quarter-circles, from largest to smallest, were: 2560 μm,

1280 μm, 640 μm, 600 μm, 300 μm, 150 μm, and 75 μm. The height of all of the channels in the device was 55 μm.[44]

We fabricated our microfluidic devices using standard techniques of soft lithography.[29] We used standard photolithography to pattern features of SU-8 photoresist (Microchem Corp., Newton, MA, USA) in relief on a silicon wafer (Silicon Sense, Inc., Nashua, NH, USA). This silicon master then served as a template for molding devices in poly(dimethyl siloxane) (PDMS, Dow Corning Sylgard 184, Corning, NY, USA). To prevent PDMS from adhering to the master during the molding process, we exposed the master to tridecafluoro(1,1,2,2 tetrahydroooctyl) trichlorosilane (Gelest, Inc., Philadelphia, PA, USA) under vacuum.

To create PDMS devices from the master, we casted PDMS prepolymer against the silicon master, and cured the PDMS for 3 h at 60 °C. Once the PDMS had cured, we removed the PDMS slab from the master and punched inlet and outlet holes using a circular biopsy punch (1.5 mm diameter, Shoney Scientific Inc., Waukesha, WI, USA). We sealed the PDMS slab to either a glass slide (50 × 75 mm, 1.2 mm thick, VWR) or a glass coverslip (48 × 65 mm, No. 1 thickness, Gold Seal® Cover Glass, Fisher Scientific Co., Boston, MA, USA) by exposing the surfaces of the glass and the PDMS slab to an air plasma for five minutes and one minute, respectively. This process oxidized the surfaces, and rendered them hydrophilic. By placing the oxidized surfaces in contact, we created an irreversible, covalent seal between the PDMS and the glass substrate. After sealing the surfaces together, we placed the device in an oven for 10 min at 60 °C to allow the surfaces to bond completely. We then immediately filled the channels of the device with liquid (water or M9 buffer) to prevent the channels from reverting to the hydrophobic state.[45]

Preparing NGM plates seeded with bacteria

Saturated cultures of *E. coli* (OP50) were grown by inoculating 10 mL of LB medium (10 g L^{-1} tryptone, 5 g L^{-1} yeast extract, 5 g L^{-1} NaCl, 1 mL 1 M NaOH) with *E. coli* and incubating the culture for 16 h at 37 °C. We seeded NGM plates with bacteria by adding 2–3 mL of saturated OP50 to each plate and leaving the plates at room temperature for 2–3 days.

Maintenance of *C. elegans*

Wild-type (N2) strains of *C. elegans* were obtained from the Caenorhabditis Genetics Center at the University of Minnesota (St. Paul). Worms were grown at 20 °C on NGM agar that had been previously seeded with the OP50 strain of *E. coli* (food source).[37] Worms were transferred to fresh plates of NGM with *E. coli* every 7–10 days to maintain healthy (not starved) stocks of worms.

Preparation of synchronous worms

We prepared populations of synchronous worms as described in the literature.[37] We transferred approximately 25 gravid (egg-containing) adult worms from a bacterial lawn into a small volume (0.5 mL) of a 1 : 1 mixture of 1 M sodium hydroxide and sodium hypochlorite on an unseeded NGM plate. Within 10 min, the alkaline hypochlorite solution had dissolved the bodies of the adult worms; the developing embryos within the adult worms, however, are encased in chitinous shells, which protect them from damage.[38]

The eggs that were released were collected from the NGM plate using 1 mL of M9 buffer per plate. The suspension of eggs was centrifuged at 1300 × *g* for 30 s. The supernatant liquid was removed and replaced by fresh M9 buffer. This washing step was repeated two times.

We incubated the eggs at 20 °C in M9, without food, overnight to allow eggs to hatch into the first larval stage (L1). The next morning, we transferred the L1 worms to NGM plates containing *E. coli*, and incubated them at 20 °C for approximately 45 h, to allow them to reach the young adult stage.

Monitoring survival in *C. elegans*

We monitored the lifespans of the worms by observing each day whether or not the animals moved in response to being touched with a platinum wire.[41] Worms that did not move were scored as dead. Worms were removed from the analysis of lifespans if they were lost during incubation. (Worms occasionally crawl off of the agar and onto the side of the polystyrene petri dish in which they are incubated. These worms usually die from desiccation.) During the first week following removal of the worms from the device, we transferred the worms to fresh plates every day in order to separate the worms from their progeny.

Acknowledgements

This research was supported by the Department of Energy (DoE) under award no. DE-FGO2-OOER45852. This work was performed in part at the Center for Nanoscale Systems (CNS), a member of the National Nanotechnology Infrastructure Network (NNIN), which is supported by the National Science Foundation under NSF award no. ECS-0335765. CNS is part of the Faculty of Arts and Sciences at Harvard University. S.E.H. gratefully acknowledges a National Defense Science and Engineering Graduate (NDSEG) Fellowship from the American Society for Engineering Education (ASEE).

References

1 L. Avery and B. B. Shtonda, *J. Exp. Biol.*, 2003, **206**, 2441–2457.
2 D. K. Chow, C. F. Glenn, J. L. Johnston, I. G. Goldberg and C. A. Wolkow, *Exp. Gerontol.*, 2006, **41**, 252–260.
3 S. Chung, D. Clark, C. Gabel, E. Mazur and A. Samuel, *BMC Neurosci.*, 2006, **7**, 30.
4 M. F. Yanik, H. Cinar, H. N. Cinar, A. D. Chisholm, Y. Jin and A. Ben-Yakar, *Nature*, 2004, **432**, 822.
5 I. Mori and Y. Ohshima, *Nature*, 1995, **376**, 344–348.
6 M. A. Hilliard, A. J. Apicella, R. Kerr, H. Suzuki, P. Bazzicalupo and W. R. Schafer, *EMBO J.*, 2005, **24**, 63–72.
7 R. Kerr, V. Lev-Ram, G. Baird, P. Vincent, R. Y. Tsien and W. R. Schafer, *Neuron*, 2000, **26**, 583–594.
8 A. Miyawaki, *Curr. Opin. Neurobiol.*, 2003, **13**, 591–596.
9 M. B. Goodman, D. H. Hall, L. Avery and S. R. Lockery, *Neuron*, 1998, **20**, 763–772.
10 J. E. Richmond, in *WormBook*, ed. The *C. elegans* Research Community, WormBook, October 6, 2006.

11 J. Sulston and J. Hodgkin, in *The Nematode Caenorhabditis elegans*, ed. Community of *C. elegans* Researchers, The Nematode *Caenorhabditis elegans*, 1988.
12 J. A. Lewis, C. H. Wu, H. Berg and J. H. Levine, *Genetics*, 1980, **95**, 905–928.
13 D. M. Raizen and L. Avery, *Neuron*, 1994, **12**, 483–495.
14 D. B. Dusenbery, *J. Comp. Physiol., A*, 1980, **136**, 327–331.
15 N. Kim, C. M. Dempsey, J. V. Zoval, J.-Y. Sze and M. J. Madou, *Sens. Actuators, B*, 2007, **122**, 511.
16 D. Lange, C. W. Storment, C. A. Conley and G. T. A. Kovacs, *Sens. Actuators, B*, 2005, **107**, 904.
17 X. Heng, D. Erickson, L. R. Baugh, Z. Yaqoob, P. W. Sternberg, D. Psaltis and C. Yang, *Lab Chip*, 2006, **6**, 1274–1276.
18 Z. F. Altun and D. H. Hall, 2005, Handbook of *C. elegans* Anatomy, in *WormAtlas*. http://www.wormatlas.org/handbook/contents.htm.
19 N. A. Croll, *J. Zool.*, 1975, **176**, 159–176.
20 J. Karbowski, C. J. Cronin, A. Seah, J. E. Mendel, D. Cleary and P. W. Sternberg, *J. Theor. Biol.*, 2006, **242**, 652–669.
21 W. Geng, P. Cosman, C. C. Berry, Z. Feng and W. R. Schafer, *IEEE Trans. Biomed. Eng.*, 2004, **51**, 1811–1820.
22 J.-H. Baek, P. Cosman, Z. Feng, J. Silver and W. R. Schafer, *J. Neurosci. Methods*, 2002, **118**, 9–21.
23 S. C. Gifford, J. Derganc, S. S. Shevkoplyas, T. Yoshida and M. W. Bitensky, *Br. J. Haematol.*, 2006, **135**, 395–404.
24 S. C. Gifford, M. G. Frank, J. Derganc, C. Gabel, R. H. Austin, T. Yoshida and M. W. Bitensky, *Biophys. J.*, 2003, **84**, 623–633.
25 M. J. Fuerstman, A. Lai, M. E. Thurlow, S. S. Shevkoplyas, H. A. Stone and G. M. Whitesides, *Lab Chip*, 2007, DOI: 10.1039/b706549c.
26 D. B. Weibel, W. R. DiLuzio and G. M. Whitesides, *Nat. Rev. Microbiol.*, 2007, **5**, 209–218.
27 D. B. Weibel and G. M. Whitesides, *Curr. Opin. Chem. Biol.*, 2006, **10**, 584.
28 Y. Xia and G. M. Whitesides, *Angew. Chem., Int. Ed.*, 1998, **37**, 550–575.
29 S. K. Sia and G. M. Whitesides, *Electrophoresis*, 2003, **24**, 3563–3576.
30 G. M. Whitesides, E. Ostuni, S. Takayama, X. Jiang and D. E. Ingber, *Annu. Rev. Biomed. Eng.*, 2001, **3**, 335–373.
31 J. N. Lee, X. Jiang, D. Ryan and G. M. Whitesides, *Langmuir*, 2004, **20**, 11684–11691.
32 D. B. Weibel, P. Garstecki and G. M. Whitesides, *Curr. Opin. Neurobiol.*, 2005, **15**, 560–567.
33 A. C. Siegel, S. S. Shevkoplyas, D. B. Weibel, D. A. Bruzewicz, A. W. Martinez and G. M. Whitesides, *Angew. Chem., Int. Ed.*, 2006, **45**, 6877–6882.
34 T. Thorsen, S. J. Maerkl and S. R. Quake, *Science*, 2002, **298**, 580–584.
35 D. B. Weibel, M. Kruithof, S. Potenta, S. K. Sia, A. Lee and G. M. Whitesides, *Anal. Chem.*, 2005, **77**, 4726–4733.
36 D. V. Vezenov, B. T. Mayers, R. S. Conroy, G. M. Whitesides, P. T. Snee, Y. Chan, D. G. Nocera and M. G. Bawendi, *J. Am. Chem. Soc.*, 2005, **127**, 8952–8953.
37 T. Stiernagle, in *WormBook*, ed. The *C. elegans* Research Community, WormBook, February 11, 2006.
38 D. Fay, in *WormBook*, ed. The *C. elegans* Research Community, WormBook, February 17, 2006.
39 S. van den Heuvel, in *WormBook*, ed. The *C. elegans* Research Community, WormBook, September 21, 2005.
40 W. R. Schafer, in *WormBook*, ed. The *C. elegans* Research Community, WormBook, June 2, 2006.
41 T. E. Johnson and W. B. Wood, *Proc. Natl. Acad. Sci. U. S. A.*, 1982, **79**, 6603–6607.
42 M. R. Klass, *Mech. Ageing Dev.*, 1977, **6**, 413–429.
43 A. Nagy, N. Perrimon, S. Sandmeyer and R. Plasterk, *Nat. Genet.*, 2003, **33**, 276–284.
44 We are willing to provide samples of this system for research use for a limited time at no cost. Requests should be addressed to ehulme@gmwgroup.harvard.edu, and will be considered on a case-by-case basis.
45 J. N. Lee, C. Park and G. M. Whitesides, *Anal. Chem.*, 2003, **75**, 6544–6554.